nature chemical biology

BRIEF COMMUNICATION

https://doi.org/10.1038/s41589-019-0433-0

# Regulation of PTP1B activation through disruption of redox-complex formation

Avinash D. Londhe[1,7], Alexandre Bergeron[2,3,7], Stephanie M. Curley[1], Fuming Zhang[4], Keith D. Rivera[5], Akaash Kannan[1], Gérald Coulis[1,3], Syed H. M. Rizvi[1], Seung Jun Kim[6], Darryl J. Pappin[5], Nicholas K. Tonks[5], Robert J. Linhardt[4] and Benoit Boivin[1,2,3,5*]

**We have identified a molecular interaction between the reversibly oxidized form of protein tyrosine phosphatase 1B (PTP1B) and 14-3-3ζ that regulates PTP1B activity. Destabilizing the transient interaction between 14-3-3ζ and PTP1B prevented PTP1B inactivation by reactive oxygen species and decreased epidermal growth factor receptor phosphorylation. Our data suggest that destabilizing the interaction between 14-3-3ζ and the reversibly oxidized and inactive form of PTP1B may establish a path to PTP1B activation in cells.**

Protein tyrosine phosphatases (PTPs) are transiently inactivated in response to regulated and localized rises in reactive oxygen species (ROS) in cells[1,2]. It is increasingly apparent that controlling the catalytic activity of members of the PTP family by reversible oxidation facilitates phospho-dependent signaling and that dysregulated PTP inactivation by oxidation contributes to the etiology of a spectrum of human diseases[2–5]. PTP1B has given us important insights on the catalytic function and redox regulation of members of the PTP family[6,7]. The reversible oxidation of PTP1B leads to profound structural changes at the active site[8,9] that can be taken advantage of by conformation sensor antibodies (scFv45) to stabilize its inactive form[10]. Since stabilization of the oxidized, inactive form of PTP1B (PTP1B-OX) by scFv45 perturbs the normal role of PTP1B on signaling pathways, we enquired whether a protein having a similar function existed in vivo.

A comparative study between the crystal structure of the inactive sulfenyl-amide species of PTP1B-OX and reduced PTP1B (PTP1B-R) revealed that a sequence of ten amino acids of the phospho-tyrosine (pTyr) recognition loop, reported to bind scFv45 (ref. [11]), were newly exposed to the cytosol in the inactive form of PTP1B in addition to the changes in the PTP loop[10] (Fig. 1a,b and Supplementary Fig. 1a). We calculated the surface accessible area of these cytosol-exposed amino acids (Supplementary Fig. 1b) and we hypothesized that this loop could recruit redox-specific PTP1B-binding proteins in cells. Therefore, a peptide comprising PTP1B amino acids Lys$^{41}$ to Ser$^{50}$ was synthetized and used as bait in cells. We used isobaric mass tags and liquid chromatography–tandem MS to quantify and identify those proteins that interacted with the pTyr loop-derived peptides and pulled down from cellular extracts. 14-3-3ζ was one of the most abundant proteins, and the most abundant 14-3-3 isoform, found interacting with the pTyr loop-derived peptide when compared with the control beads (Supplementary Tables 1 and 2, isobaric tag for relative and absolute quantitation (iTRAQ): NP (non-phosphorylated pTyr loop-derived peptide-conjugated beads) versus C (cysteine-conjugated beads) lane). Enrichment of 14-3-3ζ was even more pronounced when a PTP1B-derived peptide comprising the sequence from Lys$^{41}$ to Ser$^{50}$ was phosphorylated on Ser$^{50}$ and used as bait in cellular extracts.

The crystal structure of 14-3-3ζ revealed a conserved amphipathic groove that allows 14-3-3s to associate with proteins in a phosphorylation-dependent and -independent manner to perform a range of functions that includes altering their activity, their association with other molecules or their subcellular localization[12,13]. Optimal 14-3-3 binding motifs contain an arginine residue in the −2 to −5 position from the phospho-serine/threonine residue and a proline residue in the +2 position[13]. On examination of the pTyr recognition loop sequence, we identified a noncanonical 14-3-3 binding motif containing an arginine residue in the −3 position and a proline in the +1 position (Supplementary Fig. 2). While the pTyr recognition loop is one of the conserved motifs that define the PTP family, the residues flanking this motif vary between members of the PTP family[14]; in particular, the Ser residue (Ser$^{50}$ in PTP1B) is only preserved in three members of the PTP family (Supplementary Fig. 3). To assess the ability of 14-3-3ζ to interact with PTP1B-OX in cells, we tested whether wild-type PTP1B coimmunoprecipitated with 14-3-3ζ following epidermal growth factor receptor (EGFR) activation. Using this well-characterized signaling pathway that leads to a rapid increase in ROS production and PTP1B inactivation[3,15], we first established that PTP1B was reversibly oxidized using a cysteinyl-labeling assay that converts reversible oxidation of the catalytic cysteine of PTPs to a modification by biotin that can be visualized by immunoblotting after a biotin-streptavidin purification step (Fig. 1c and Supplementary Fig. 4)[16,17]. As shown in Fig. 1c, minimal PTP1B oxidation was detected in resting cells; however, PTP1B biotinylation was detected in a transient manner at 1 and 2 min following EGFR activation. Supporting our MS data, immunoprecipitations revealed a transient association between PTP1B and 14-3-3ζ between 2 and 5 min following EGFR activation (Supplementary Fig. 5a,b). This transient interaction between PTP1B and 14-3-3ζ was detected in coimmunoprecipitations of either endogenously (Supplementary Fig. 6) or exogenously expressed PTP1B and 14-3-3ζ from lysates of cells stimulated with epidermal growth factor (EGF). Detection of some association between endogenous PTP1B and 14-3-3ζ in unstimulated cells (Supplementary Fig. 6) is likely the result of increased

[1]Department of Nanobioscience, College of Nanoscale Science and Engineering, SUNY Polytechnic Institute, Albany, NY, USA. [2]Department of Medicine, Université de Montréal, Montreal, Quebec, Canada. [3]Montreal Heart Institute, Montreal, Quebec, Canada. [4]Department of Chemistry and Chemical Biology, Center for Biotechnology and Interdisciplinary Studies, Rensselaer Polytechnic Institute, Troy, NY, USA. [5]Cold Spring Harbor Laboratory, Cold Spring Harbor, NY, USA. [6]Division of Biomedical Sciences, Korea Research Institute of Bioscience & Biotechnology, Daejeon, Korea. [7]These authors contributed equally: Avinash D. Londhe, Alexandre Bergeron. *e-mail: bboivin@sunypoly.edu

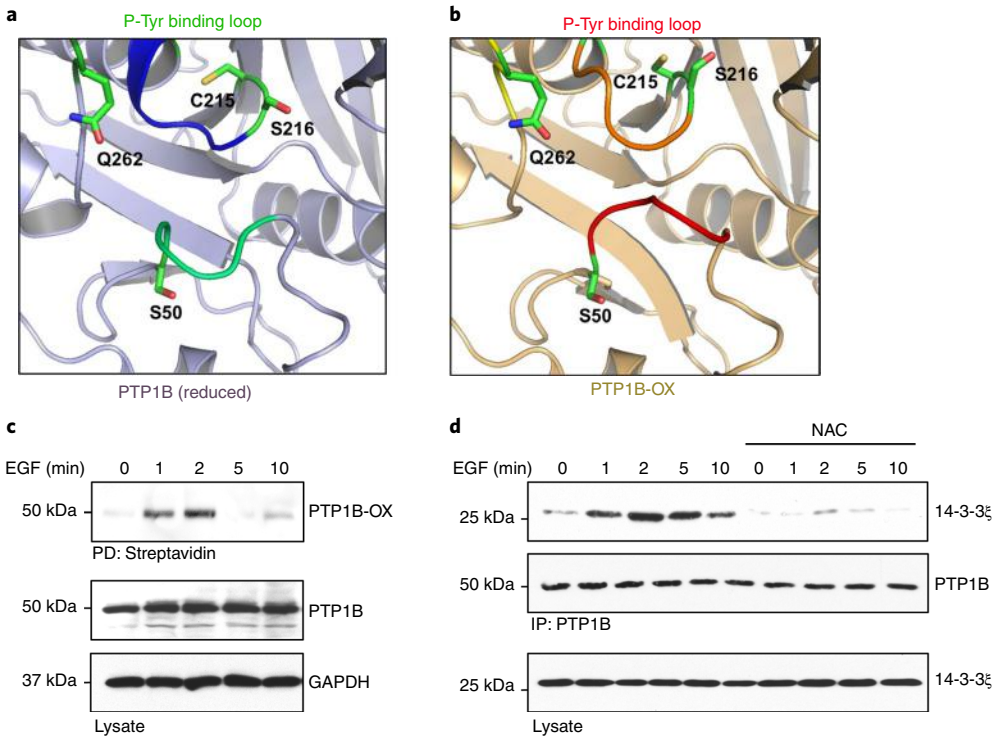


**Fig. 1 | The exposed pTyr recognition loop of PTP1B-OX interacts with 14-3-3ζ. a**,**b**, Close-up view of the pTyr recognition loop of PTP1B-R (PDB code: 2HNQ) (**a**) and of PTP1B-OX (sulfenyl-amide species, PDB code: 1OEM) (**b**). **c**, Reversible oxidation of PTP1B in cells treated with EGF (100 ng ml$^{-1}$) for the indicated times. This experiment was repeated three independent times with representative data shown. **d**, Effect of scavenging ROS on the PTP1B–14-3-3ζ association in cells incubated with the antioxidant NAC (1 mM, 1 h) and stimulated with EGF for the indicated times. This experiment was repeated two independent times with representative data shown. Uncropped images are shown in Supplementary Fig. 12.

protein input in the coimmunoprecipitations to compensate for a decreased dynamic range in the assay. Redox-dependent association between PTP1B and 14-3-3ζ was confirmed by pre-incubating cells with the antioxidant N-acetylcysteine (NAC) before EGF stimulation (Fig. 1d). Interestingly, the mitochondrial antioxidant SS-31 did not prevent the association between PTP1B and 14-3-3ζ, and a mutant PTP1B that adopts an oxidized conformation (PTP1B$^{CASA}$ (ref. [10])) interacted with 14-3-3ζ despite antioxidant pretreatments (Supplementary Fig. 7). Thus, 14-3-3ζ is shown to specifically interact with an oxidized PTP in cells.

To further understand the function of the interaction between PTP1B-OX and 14-3-3ζ, and to determine whether this interaction regulates the redox status of PTP1B, we directly prevented 14-3-3ζ binding to PTP1B using the pan 14-3-3 inhibitor peptide R18 (ref. [18]). This peptide binds the amphipathic groove of 14-3-3s and competes with endogenous ligands. As expected, inhibiting 14-3-3s by exposing cells to R18 prevented the interaction between 14-3-3ζ and PTP1B (Fig. 2a). However, the cysteinyl-labeling assay also revealed that R18 prevented biotinylation of PTP1B, which reflects the reversible oxidation of PTP1B in cells (Fig. 2b). Since Ser$^{50}$ of the pTyr recognition loop of PTP1B is buried in the structure of the reduced enzyme (Fig. 1a,b and Supplementary Fig. 1), we hypothesized that when the pTyr recognition loop becomes exposed to the cytosol as a consequence of PTP1B oxidation, Ser$^{50}$ becomes accessible and readily phosphorylated by AKT/protein kinase B, a protein kinase known to phosphorylate PTP1B on this residue[19]. Hence, we investigated whether the reversible oxidation of PTP1B occurred as a consequence of Ser$^{50}$ phosphorylation and the subsequent association with 14-3-3ζ. Exposing cells to an AKT inhibitor (that is, AKT inhibitor V/API-2 (ref. [20])) prevented phosphorylation of AKT Ser$^{473}$ and PTP1B Ser$^{50}$ following EGF stimulation (Supplementary Fig. 8a). Similar to our previous observation using a 14-3-3 inhibitor, preventing PTP1B phosphorylation on Ser$^{50}$ impaired the interaction between PTP1B and 14-3-3ζ and compromised the reversible oxidation of PTP1B (Supplementary Fig. 8b,c). This is consistent with a mechanism in which the interaction between 14-3-3ζ and PTP1B stabilizes PTP1B-OX in cells.

To gain some insight on the nature of the interaction between PTP1B and 14-3-3ζ, we next tested whether the interaction between 14-3-3ζ and PTP1B was a direct protein–protein interaction. As a first step, we performed an in vitro pulldown experiment and observed that while 14-3-3ζ interacted with PTP1B-OX when phosphorylated on Ser$^{50}$ (phosphoPTP1B-OX, PTP1B-OX(P)), no interaction occurred with PTP1B-R (Supplementary Fig. 9a,b). We then analyzed the molecular interaction between 14-3-3ζ and PTP1B-OX(P) by surface plasmon resonance (SPR) and confirmed that 14-3-3ζ specifically binds to PTP1B in its oxidized and phosphorylated inactive state but not to the active reduced form of the enzyme (Fig. 2c), consistent with the interaction observed in cells. The dependency on phosphorylation of Ser$^{50}$ for 14-3-3ζ binding was further confirmed by SPR using immobilized phosphoSer$^{50}$ (pSer50)-pTyr loop-derived peptide (Supplementary Fig. 9c). Moreover, real-time binding of increasing concentrations of 14-3-3ζ and a fixed amount of PTP1B-OX(P) indicated that binding occurred with high affinity (equilibrium constant, $K_D$: 79 nM) and a relatively slow off-rate (dissociation rate constant, $K_{off} = 4.58 \times 10^{-3}\ s^{-1}$) (Supplementary Fig. 9d). These SPR results support a model in which 14-3-3ζ directly binds to the pTyr recognition loop of PTP1B in a pSer$^{50}$-dependent fashion, and reveal that the interaction between 14-3-3ζ and the unphosphorylated pTyr recognition loop peptide that was previously observed by MS analysis (Supplementary Tables 1 and 2) occurs indirectly via a protein intermediate.

The cysteinyl-labeling assay is an approach that allows us to measure PTP1B inactivation by reversible oxidation (Supplementary

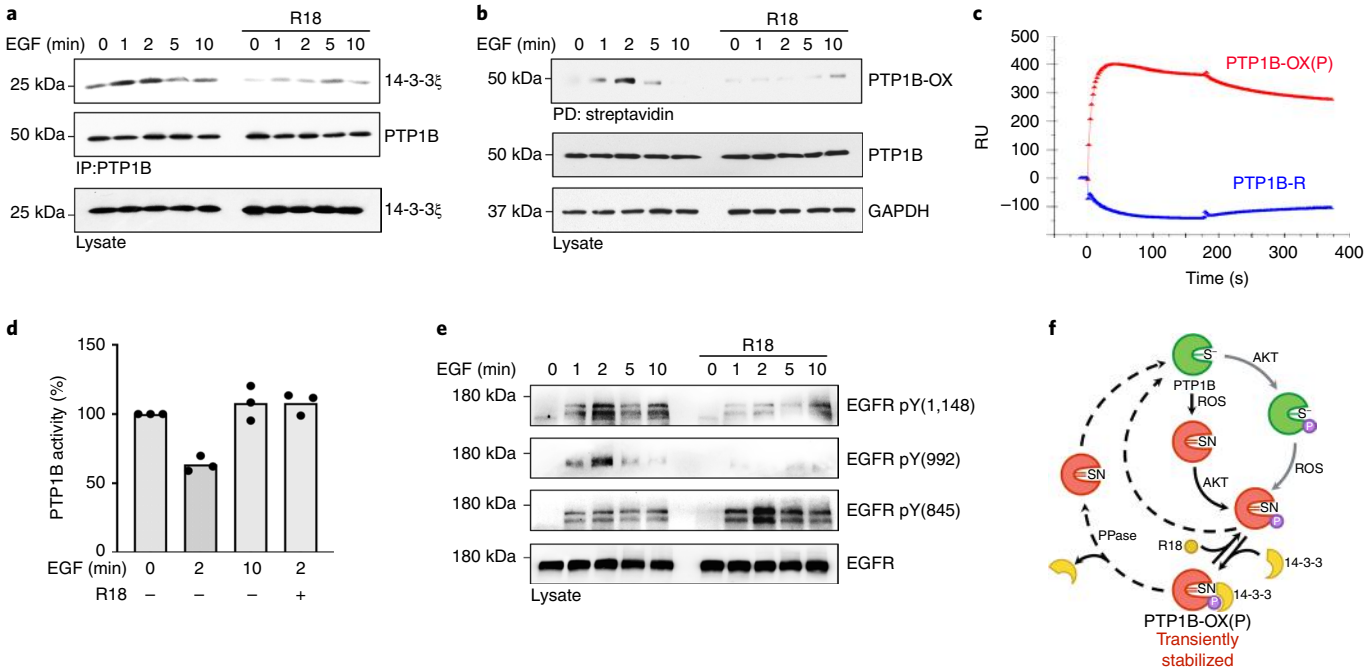


**Fig. 2 | Destabilizing the association between 14-3-3ζ and PTP1B-OX prevents PTP1B inactivation and decreases EGFR phosphorylation. a**, Effect of exposing cells to the 14-3-3 inhibitor peptide R18 (25 μM, 90 min) on the transient interaction between PTP1B and 14-3-3ζ. Uncropped images are shown in Supplementary Fig. 13a. This experiment was repeated three independent times with representative data shown. **b**, Reversible-oxidation of PTP1B was measured following R18 pretreatment using the cysteinyl-labeling assay. Uncropped images are shown in Supplementary Fig. 13b. This experiment was repeated three independent times with representative data shown. **c**, Comparative SPR sensorgram of the interaction between 14-3-3ζ (5,000 nM) and either PTP1B-OX(P) (red) or PTP1B-R (blue) showing direct association between PTP1B-OX(P) and 14-3-3ζ. **d**, Quantitative analysis of PTP1B catalytic activity from immune-complexes, showing the effects of preventing PTP1B association with 14-3-3ζ using R18 before cell exposure to EGF for the indicated times. The average readout value of technical replicates is represented by the dot-plot bar graph. $N = 3$ independent experiments are shown. **e**, Effect of pretreating cells with R18 on EGFR tyrosine phosphorylation. Phosphorylation of EGFR on PTP1B sites (pTyr$^{992}$ and pTyr$^{1148}$) was decreased, whereas phosphorylation of EGFR on Tyr$^{845}$ was increased. Uncropped images are shown in Supplementary Fig. 14. This experiment was repeated three independent times with representative data shown. **f**, The proposed mechanism leading to transient stabilization of PTP1B oxidation in cells is indicated with black arrows. In resting cells, PTP1B is active (green) and possesses a reactive catalytic cysteine residue ($S^-$). Following EGFR activation, a ROS-producing stimulus, PTP1B becomes rapidly and transiently inactivated by ROS (red). Key conformational changes of the inactive sulfenyl-amide (SN) species of PTP1B-OX include one element of the active site, the pTyr recognition loop containing the sequence Lys$^{41}$ to Ser$^{50}$. In the structure of PTP1B-OX, this loop adopts a cytosol-exposed position and becomes phosphorylated on Ser$^{50}$ by AKT, which leads to 14-3-3 binding. In turn, binding of 14-3-3 to PTP1B-OX(P) transiently stabilizes the inactive, oxidized form of the enzyme and allows phosphorylation of its substrates. Alternatively, preventing the transient interaction between 14-3-3 and PTP1B-OX using R18 perturbed the redox cycle of PTP1B and effectively prevented PTP1B inactivation by ROS. Reactivation mechanisms for PTP1B, involving an unidentified pSer$^{50}$ phosphatase, thioredoxin[24] or cellular thiols[25], and alternative inactivation mechanisms, are indicated with dashed and gray arrows, respectively. PPase, phosphatase; pY, phospho-tyrosine; RU, resonance units.

Fig. 4). Decreased biotinylation of PTP1B observed in the cysteinyl-labeling assay when cells are exposed to R18 could reflect either the absence of PTP1B oxidation, or irreversible oxidation of the catalytic cysteine residue to sulfinic or sulfonic forms. To determine whether disrupting the interaction between 14-3-3ζ and PTP1B decreased reversible oxidation of PTP1B, we measured PTP1B catalytic activity in lysates from EGF-stimulated cells that were pretreated with R18 or not. PTP1B was immunoprecipitated from lysates in oxygen-free conditions to minimize postlysis oxidation of the phosphatase and the catalytic activity of PTP1B was then measured using the pTyr analog, pNPP, as substrate. As expected from previous studies, PTP1B activity was greatly decreased in lysates from cells exposed to EGF for 2 min (36.3% ± 5.6%), and mostly recovered after 10 min (Fig. 2d). However, PTP1B maintained maximal catalytic activity after 2 min of EGF stimulation in cells that were pretreated with R18, indicating that PTP1B remains active in R18-treated cells, when the PTP1B-OX(P)–14-3-3ζ complex is disrupted. Measuring the activity of PTP1B from the same lysates in reducing conditions confirmed that decreased enzymatic activity after EGF stimulation occurred as a consequence of reversible oxidation (Supplementary Fig. 10).

Given that R18 hindered binding of 14-3-3ζ onto PTP1B-OX(P) and maintained PTP1B in an active state, we tested whether preventing transient PTP1B oxidation had an impact on EGFR tyrosine phosphorylation and activation. Immunoprecipitation of pTyr proteins and immunoblotting with anti-EGFR antibodies showed that pretreating cells with R18 before EGF exposure did not affect the overall phosphorylation of EGFR (Supplementary Fig. 11). In contrast, when monitoring phosphorylation of EGFR at two specific sites, tyrosine 992 and tyrosine 1148, two sites previously reported to be direct substrates of PTP1B (ref. [21]), phosphorylation was markedly decreased in EGF-stimulated cells pretreated with R18 (Fig. 2e). On the other hand, EGFR phosphorylation at tyrosine 845, an SRC kinase phosphorylation site[22], was increased, consistent with PTP1B-mediated SRC activation[23]. Collectively, our data support that destabilizing protein interaction between the oxidized and phosphorylated, inactive form of PTP1B and 14-3-3 with appropriate therapeutic molecules allows rapid reactivation of PTP1B and may be used to limit excessive growth factor signaling pathways involving PTP1B (Fig. 2f). The concept that stabilization of PTP1B oxidation is necessary to maintain the enzyme in an inactive form

may be broadly applicable to redox-regulated enzymes and offer a paradigm for drugs that activate PTPs.

## Online content

Any methods, additional references, Nature Research reporting summaries, source data, extended data, supplementary information, acknowledgements, peer review information; details of author contributions and competing interests; and statements of data and code availability are available at https://doi.org/10.1038/s41589-019-0433-0.

Received: 25 June 2018; Accepted: 14 November 2019;
Published online: 23 December 2019

## References

1. Finkel, T. Signal transduction by reactive oxygen species. *J. Cell Biol.* **194**, 7–15 (2011).
2. Ostman, A., Frijhoff, J., Sandin, A. & Böhmer, F. D. Regulation of protein tyrosine phosphatases by reversible oxidation. *J. Biochem.* **150**, 345–356 (2011).
3. Tonks, N. K. Protein tyrosine phosphatases: from genes, to function, to disease. *Nat. Rev. Mol. Cell Biol.* **7**, 833–846 (2006).
4. Karisch, R. et al. Global proteomic assessment of the classical protein-tyrosine phosphatome and "Redoxome". *Cell* **146**, 826–840 (2011).
5. Brown, D. I. & Griendling, K. K. Regulation of Signal Transduction by Reactive Oxygen Species in the Cardiovascular System. *Circ. Res.* **116**, 531–549 (2015).
6. Tonks, N. K. PTP1B: from the sidelines to the front lines! *FEBS Lett.* **546**, 140–148 (2003).
7. Feldhammer, M., Uetani, N., Miranda-Saavedra, D. & Tremblay, M. L. PTP1B: a simple enzyme for a complex world. *Crit. Rev. Biochem. Mol. Biol.* **48**, 430–445 (2013).
8. Salmeen, A. et al. Redox regulation of protein tyrosine phosphatase 1B involves a sulphenyl-amide intermediate. *Nature* **423**, 769–773 (2003).
9. van Montfort, R. L., Congreve, M., Tisi, D., Carr, R. & Jhoti, H. Oxidation state of the active-site cysteine in protein tyrosine phosphatase 1B. *Nature* **423**, 773–777 (2003).
10. Haque, A., Andersen, J. N., Salmeen, A., Barford, D. & Tonks, N. K. Conformation-sensing antibodies stabilize the oxidized form of PTP1B and inhibit its phosphatase activity. *Cell* **147**, 185–198 (2011).
11. Krishnan, N. et al. Harnessing insulin- and leptin-induced oxidation of PTP1B for therapeutic development. *Nat. Commun.* **9**, 283 (2018).
12. Zhao, J., Meyerkord, C. L., Du, Y., Khuri, F. R. & Fu, H. 14-3-3 proteins as potential therapeutic targets. *Semin. Cell Dev. Biol.* **22**, 705–712 (2011).
13. Reinhardt, H. C. & Yaffe, M. B. Phospho-Ser/Thr-binding domains: navigating the cell cycle and DNA damage response. *Nat. Rev. Mol. Cell Biol.* **14**, 563–580 (2013).
14. Andersen, J. N. et al. Structural and evolutionary relationships among protein tyrosine phosphatase domains. *Mol. Cell Biol.* **21**, 7117–7136 (2001).
15. Lee, S. R., Kwon, K. S., Kim, S. R. & Rhee, S. G. Reversible inactivation of protein-tyrosine phosphatase 1B in A431 cells stimulated with epidermal growth factor. *J. Biol. Chem.* **273**, 15366–15372 (1998).
16. Boivin, B., Zhang, S., Arbiser, J. L., Zhang, Z. Y. & Tonks, N. K. A modified cysteinyl-labeling assay reveals reversible oxidation of protein tyrosine phosphatases in angiomyolipoma cells. *Proc. Natl Acad. Sci. USA* **105**, 9959–9964 (2008).
17. Boivin, B., Yang, M. & Tonks, N. K. Targeting the reversibly oxidized protein tyrosine phosphatase superfamily. *Sci. Signal.* **3**, pl2 (2010).
18. Wang, B. et al. Isolation of high-affinity peptide antagonists of 14-3-3 proteins by phage display. *Biochemistry* **38**, 12499–12504 (1999).
19. Ravichandran, L. V., Chen, H., Li, Y. & Quon, M. J. Phosphorylation of PTP1B at Ser(50) by Akt impairs its ability to dephosphorylate the insulin receptor. *Mol. Endocrinol.* **15**, 1768–1780 (2001).
20. Yang, L. et al. Akt/protein kinase B signaling inhibitor-2, a selective small molecule inhibitor of Akt signaling with antitumor activity in cancer cells overexpressing Akt. *Cancer Res.* **64**, 4394–4399 (2004).
21. Milarski, K. L. et al. Sequence specificity in recognition of the epidermal growth factor receptor by protein tyrosine phosphatase 1B. *J. Biol. Chem.* **268**, 23634–23639 (1993).
22. Biscardi, J. S. et al. c-Src-mediated phosphorylation of the epidermal growth factor receptor on Tyr845 and Tyr1101 is associated with modulation of receptor function. *J. Biol. Chem.* **274**, 8335–8343 (1999).
23. Lessard, L., Stuible, M. & Tremblay, M. L. The two faces of PTP1B in cancer. *Biochim. Biophys. Acta* **1804**, 613–619 (2010).
24. Dagnell, M. et al. Selective activation of oxidized PTP1B by the thioredoxin system modulates PDGF-β receptor tyrosine kinase signaling. *Proc. Natl Acad. Sci. USA* **110**, 13398–13403 (2013).
25. Parsons, Z. D. & Gates, K. S. Thiol-dependent recovery of catalytic activity from oxidized protein tyrosine phosphatases. *Biochemistry* **52**, 6412–6423 (2013).

## Methods

**Materials.** Anti-EGFR, GAPDH and 14-3-3ζ were from Santa Cruz Biotechnology. Anti-Pan-AKT, anti-AKT pSer$^{473}$ and anti-phosphoEGFR antibodies were from Cell Signaling Technology. HA-peroxidase and anti-PTP1B (FG6) were from Millipore. PT-66-agarose-conjugated beads, anti-FLAG M2 beads, anti-HA beads and anti-Flag M2 peroxidase were purchased from Sigma. Anti-PTP1B pSer$^{50}$ (Ab62320) was from Abcam. Streptavidin-HRP was from GE Healthcare. HRP-conjugated secondary antibodies were from Jackson ImmunoResearch Laboratories. Protease inhibitor mixture tablets were from Roche. Catalase and superoxide dismutase were from Calbiochem. Surfact-Amps Nonidet P-40, Zeba desalt spin columns, EZ-Link biotin-iodoacetyl-PEG2 (biotin-IAP) and iodoacetic acid were from Thermo Scientific. The pTyr loop-derived peptide (CKNRNRYRDVS) and pSer$^{50}$ pTyr loop-derived peptide (CKNRNRYRDVpS) were from GenScript. BIACore sensor nitrilotriacetic acid (NTA) and streptavidin chips were from GE Healthcare.

**Cell culture.** HEK293T cells were maintained in culture at 40–90% confluency in Eagle's minimum essential medium (EMEM, 1,000 mg l$^{-1}$ glucose, ATCC) containing 100 U ml$^{-1}$ penicillin, 100 µg ml$^{-1}$ streptomycin and 10% FBS at 5% $CO_2$ and 37 °C. Plasmid DNA (4 µg) was routinely transfected using TurboFect (ThermoFisher) on 80% confluent cells. Transient expression was allowed to progress for 48 h. Cells were serum starved overnight using EMEM without serum.

**Assay of PTP oxidation.** The cysteinyl-labeling assay was performed as described[16,17]. In brief, cells were starved for 16 h in serum-free EMEM. For EGF stimulations, cells were stimulated with 100 ng ml$^{-1}$ EGF for indicated times and lysed in degassed lysis buffer (50 mM sodium acetate (pH 5.5), 150 mM NaCl, 1% NP40, 10% (v/v) glycerol) supplemented with 25 µg ml$^{-1}$ aprotinin, 25 µg ml$^{-1}$ leupeptin, 10 mM IAA, 250 U ml$^{-1}$ catalase and 125 U ml$^{-1}$ superoxide dismutase, after which alkylation was allowed for 1 h at room temperature. Lysates were cleared by centrifugation at 10,000 r.p.m. for 10 min, and buffer exchanged with (1 mM) Tris (2-carboxyethyl) phosphine (TCEP)-containing lysis buffer using Zeba columns (Pierce). Lysates were reduced for 30 min, and supplemented with a (5 mM) biotin-labeled iodoacetic acid probe (Pierce). Labeled PTP1B was pulled down with streptavidin–sepharose beads, boiled for 2 min in sample buffer and used for immunoblotting.

**Immunoprecipitation and immunoblotting.** FLAG-PTP1B, HA-14-3-3ζ and EGFR were immunoprecipitated as follows. Cells were grown to 80% confluence in 10-cm plates, transfected for 48 h and serum-starved for 16 h. Following serum-starvation, cells were pretreated (R18, 25 µM; AKT inhibitor V/API-2, 15 µM, 1 h; NAC, 1 mM, 1 h) or not and stimulated with EGF to activate EGFR for the indicated times. After treatment, the plates were transferred on ice, washed with cold PBS and extracted in 800 µl of a lysis buffer consisting of 20 mM HEPES pH 7.4, 150 mM NaCl, 1% NP40, 1 mM EDTA, 10 mM NaF, 25 µg ml$^{-1}$ aprotinin, 25 µg ml$^{-1}$ leupeptin, 1 µM microcystin and 100 nM okadaic acid. $Na_3VO_4$ (1 mM) was also supplemented to the lysis buffer in experiments assessing EGFR phosphorylation. All subsequent steps were carried out on ice or at 4 °C. Cells were lysed on a rotating wheel at 4 °C for 30 min. Cell debris were centrifuged at 14,000*g* for 10 min, and protein concentrations were determined. Then, 500 µg of protein was diluted in cold lysis buffer and precleared for 20 min with sepharose beads. The supernatants were incubated for 3 h on a rotating wheel with appropriate beads precoupled to –HA, –FLAG, anti-EGFR antibodies or anti-pTyr antibodies (PT-66). The immune complexes were pelleted at 3,000*g* for 5 min and washed three times with cold lysis buffer. The beads were resuspended in 20 µl of 4X Laemmli sample buffer and heated at 95 °C for 2 min. Proteins were separated by SDS–PAGE and detected by immunoblotting.

**Protein expression and in vitro Ni-NTA precipitation assay.** The interaction between PTP1B and 14-3-3ζ was performed in vitro using purified proteins. Bacterially expressed His-PTP1B (residues 1–321) and GST-14-3-3ζ were purified by Ni-NTA and agarose glutathione, respectively, and PTP1B was stored in a 1 mM TCEP solution to prevent postpurification oxidation. PTP1B was then reversibly oxidized as previously performed[10], and phosphorylated. Briefly, purified PTP1B (50 nM) was reversibly oxidized with 250 µM $H_2O_2$ in HEPES buffer (50 mM HEPES, 100 mM NaCl, pH 7.0) for 10 min at room temperature. $H_2O_2$ was then removed by buffer exchange, using desalting columns equilibrated with a modified kinase assay buffer (50 mM Tris, 10 mM $MgCl_2$, 5 mM ATP, pH 7.4) containing no reducing agent. Phosphorylation of PTP1B-OX was then initiated by the addition of AKT (in a 1:200, AKT/PTP1B-OX molar ratio) and incubated at 30 °C for 16 h. Optimal phosphorylation of PTP1B Ser$^{50}$ by AKT was established by analyzing levels of PTP1B-Ser$^{50}$ phosphorylation following incubations of 1, 3, 6 and 16 h. Direct interaction between PTP1B-OX-(P) and 14-3-3ζ was performed by incubating 50 nM PTP1B-OX(P) or PTP1B-R with 5 µM 14-3-3ζ in binding buffer (20 mM HEPES, 150 mM NaCl, 0.05% BSA, 0.05% Tween, pH 7.4) for 2 h at 4 °C on a clinical rotator. Glutathione agarose beads were added and incubated with the protein complexes for 1 h at 4 °C and protein complexes bound to glutathione agarose beads were centrifuged and washed three times for 5 min at 4 °C with binding buffer. Protein complexes were further separated by SDS–PAGE, transferred onto nitrocellulose membranes and blotted for PTP1B using anti-PTP1B (FG6) antibody, and for 14-3-3ζ using an anti-GST antibody. Protein amounts of PTP1B were scaled up 1,000-fold to generate sufficient PTP1B-OX(P) for SPR experiments.

**Preparation of protein chips for SPR experiments.** SPR binding assays were performed to assess binding of 14-3-3ζ to the pTyr recognition loop-derived peptide (cysteine-K$^{41}$NRNRYRDVS$^{50}$: linked to biotin-IAP), PTP1B-OX(P) and PTP1B-R using a BIAcore 3000 (GE Healthcare) operated using BIAcore 3000 Control and BIAevaluation software (v.4.0.1). To obtain kinetic data for Cys-K$^{41}$NRNRYRDVS$^{50}$/K$^{41}$NRNRYRDVpS$^{50}$ and 14-3-3ζ interactions, biotinylated Cys-K$^{41}$NRNRYRDVS$^{50}$ and Cys-K$^{41}$NRNRYRDVpS$^{50}$ were immobilized to the streptavidin chip based on the manufacturer's protocol. In brief, a 20-µl solution of biotin-Cys-K$^{41}$NRNRYRDVS$^{50}$ or biotin-Cys-K$^{41}$NRNRYRDVpS$^{50}$ (3.69 mM) was injected over flow cells 2 and 3 (FC2 and FC3) of the streptavidin chip at a flow rate of 10 µl min$^{-1}$. The successful immobilizations of biotinylated Cys-K$^{41}$NRNRYRDVS$^{50}$ and Cys-K$^{41}$NRNRYRDVpS$^{50}$ were confirmed by observation of 521- and 389-resonance unit increases, respectively, on the sensor chip. The control flow cell (FC1) was prepared by 1-min injection with saturated biotin.

To obtain kinetic data for PTP1B and 14-3-3ζ interactions, histidine (His)-tagged PTP1B-OX(P) and PTP1B-R were immobilized on an NTA sensor chip, which is designed to bind His-tagged molecules by relying on an NTA-chelated nickel atom, according to standard protocol (GE Healthcare). Briefly, the NTA surface was activated by injection pulse of 10 µl (flow rate, 10 µl min$^{-1}$) of 500 µM $NiCl_2$ in HEPES-buffered 150 mM NaCl (HBSN) solution (0.01 M HEPES, 0.15 M NaCl, pH 7.4). Following activation, 20 µl His-tagged PTP1B-OX(P) (2.7 µM) and PTP1B-R (2.7 µM) were injected over the activated biosensor surface. The successful immobilizations of PTP1B-OX(P) and PTP1B-R were confirmed by observation of 460- and 4,050-resonance unit increases, respectively, on the sensor chip. A reference flow cell was used with the NTA surface without $NiCl_2$ activation.

**Measurement of interactions using BIAcore.** 14-3-3ζ was diluted in HBSN buffer (0.01 M HEPES, 0.15 M NaCl, pH 7.4). Diluted 14-3-3ζ samples (indicated concentrations) were injected at a flow rate of 30 µl min$^{-1}$. At the end of the sample injection, HBSN buffer as running buffer was flowed over the sensor surface to facilitate dissociation. After a 3-min dissociation time, the sensor surface was regenerated by injecting with 30 µl 2 M NaCl, giving a fully regenerated surface. The response was monitored as a function of time (sensorgram) at 25 °C.

**PTP activity assay.** PTP1B activity assay was performed on HEK293T cells. First, 60–80% confluent cells were transfected with PTP1B-FLAG and 14-3-3ζ-HA for 48 h. Cells were serum-starved 32 h post-transfection for a 16-h period and stimulated with EGF (100 ng ml$^{-1}$) for the indicated times, in the presence or absence of R18 (25 µM, 90 min). Cells were lysed under strict hypoxic conditions on ice, followed by a cold degassed lysis buffer consisting of 25 mM HEPES pH 7.4, 150 mM NaCl, 1 mM EDTA and 1% Surfact-Amps NP40. Degassing of the buffer is a critical step for this assay. The degassing steps were based on a method previously described[16,17]. Cells were lysed on a rotating wheel at 4 °C for 30 min. Cell debris were centrifuged at 14,000*g* for 10 min, and protein concentrations were determined. The supernatants (200 µg) were incubated at 4 °C for 3 h on a rotating wheel with 10 µl anti-FLAG Dynabeads (Life Technologies). The immune complexes were then washed with degassed lysis buffer and resuspended in pNPP assay buffer (20 mM HEPES pH 7.4, 100 mM NaCl and 0.05% w/v BSA, 20 mM pNPP), with or without DTT (5 µM). The beads were protected from light on a rotator at room temperature and the converted substrate was measured following a 30-min incubation. Then, 80 µl of the supernatant from the enzymatic reaction was stopped with 20 µl 2 M NaOH, and absorbance was measured at 405 nm using a spectrophotometer (SpectraMax, Molecular Devices).

**pTyr loop-derived peptide pulldown for MS.** HEK293T cells were lysed in a lysis buffer consisting of 20 mM HEPES pH 7,4, 150 mM NaCl, 1% NP40, 1 mM EDTA, 10 mM NaF, 25 µg ml$^{-1}$ aprotinin, 25 µg ml$^{-1}$ leupeptin, 1 µM microcystin and 100 nM okadaic acid. The protein content of lysate was measured by Bradford assay, and equal amounts of lysates were incubated with the pTyr loop-derived peptide (CKNRNRYRDVS), a pSer$^{50}$ pTyr loop-derived peptide (CKNRNRYRDVpS) or L-Cys coupled to UltraLink Iodoacetyl Resin (ThermoFisher) for 90 min at 4 °C. The resin was centrifuged and washed three times with lysis buffer and three additional times with PBS. The beads were incubated with 50 µl 10 mM pTyr loop-derived peptide and pSer$^{50}$ pTyr loop-derived peptide in PBS at room temperature for 20 min to elute pTyr loop-binding proteins. The supernatants were collected and subjected to tryptic digestion and iTRAQ labeling.

**Tryptic digestion, iTRAQ labeling and dimensional fractionation.** A 1X sample volume of 10% SDS was added to eluted proteins to bring the final concentration of SDS to 5%. Next, TCEP was added to a final concentration of 5 mM and samples were heated to 55 °C for 20 min and allowed to cool to room temperature. Methyl methanethiosulfonate was added to a final concentration of 10 mM and samples were incubated at room temperature for 20 min to complete blocking of free sulfhydryl groups. A suspension-trapping (S-Trap) protocol was adapted and

used to digest proteins[26]. Briefly, lysates were acidified with phosphoric acid to a final concentration of 1.2% and added to an S-Trap containing 6X lysate volume of S-trapping buffer (90% methanol, 100 mM triethyl ammonium bicarbonate (TEAB)). S-Trap was spun down at 4,000*g* for 30 s to remove buffer, washed with 200 µl S-trapping buffer and spun again to remove all buffer. Then, 2 µg of sequencing grade trypsin (Promega) in 125 µl 50 mM TEAB was added to the S-Trap and they were digested overnight at 37 °C. After digestion, the peptides were eluted from the column with subsequent applications of 40 µl 50 mM TEAB, 40 µl 0.2% formic acid in water and 40 µl 0.2% formic acid in 50% acetonitrile. Peptides were dried in vacuo. Peptides were then reconstituted in 50 µl 0.5 M TEAB/70% ethanol and labeled with 4-plex iTRAQ reagent for 1 h at room temperature[27]. Labeled samples were then acidified to pH 4 using formic acid, combined and concentrated in vacuo until ~10 µl remained. For dimensional fractionation, peptides were fractionated using a Pierce High pH Reversed-Phase Peptide Fractionation Kit (Thermo Scientific) according to the manufacturer's instructions with slight modifications. Briefly, peptides were reconstituted in 150 µl 0.1% TFA, loaded onto the spin column and centrifuged at 3,000*g* for 2 min. The column was washed with water and then peptides were eluted with the following percentages of acetonitrile in 0.1% triethylalmine: 5%, 7.5%, 10%, 12.5%, 15%, 20%, 30% and 50%. Each of the eight fractions was then separately injected into the mass spectrometer using capillary reverse-phase liquid chromatography at low pH.

**Mass spectrometry.** An Orbitrap Fusion Lumos mass spectrometer (Thermo Scientific), equipped with a nano-ion spray source, was coupled to an EASY-nLC 1200 system (Thermo Scientific). The liquid chromatography system was configured with a self-pack PicoFrit 75-µm analytical column with an 8-µm emitter (New Objective) packed to 25 cm with ReproSil-Pur C18-AQ, 1.9 µM material (Dr. Maish GmbH). Mobile phase A consisted of 2% acetonitrile, 0.1% formic acid, and mobile phase B consisted of 90% acetonitrile, 0.1% formic acid. Peptides were then separated using the following steps: at a flow rate of 200 nl $min^{-1}$: 2% B to 6% B over 1 min, 6% B to 30% B over 84 min, 30% B to 60% B over 9 min, 60% B to 90% B over 1 min, held at 90% B for 5 min, 90% B to 50% B over 1 min, and then flow rate was increased to 500 nl $min^{-1}$ as 50% B was held for 9 min. Eluted peptides were directly electrosprayed into the Orbitrap Fusion Lumos mass spectrometer with the application of a distal 2.3-kV spray voltage and a capillary temperature of 300 °C. Full-scan mass spectrum (Resolution = 60,000; 400–1,600 $m/z$) was followed by tandem MS using the 'Top Speed' method for selection. High-energy collisional dissociation was used with the normalized collision energy set to 35 for fragmentation, with the isolation width set to 1.2, and a duration of 10 s was set for the dynamic exclusion with an exclusion mass width of 10 ppm. We used monoisotopic precursor selection for charge states 2+ and greater, and all data were acquired in profile mode.

**Database searching.** Peaklist files were generated by Mascot Distiller (Matrix Science). Protein identification and quantification were carried out using Mascot 2.6 (ref. [28]) against the UniProt human sequence database (93,799 sequences; 37,184,134 residues). Methylthiolation of cysteine and N-terminal and lysine iTRAQ modifications were set as fixed modifications, and methionine oxidation and deamidation (deamidated, NQ) as variable. Trypsin was used as cleavage enzyme with one missed cleavage allowed. Mass tolerance was set at 30 ppm for intact peptide mass and 0.2 Da for fragment ions. Search results were re-scored to give a final 1% false discovery rate using a randomized version of the same Uniprot Human database. Protein-level iTRAQ ratios were calculated as intensity weighted, using only unique peptides with expectation values < 0.0004828. As this was a protein immunoprecipitation experiment, no global ratio normalization was applied.

**Surface accessible area assessment.** The structures of PTP1B-R (PDB code: 2HNQ) and PTP1B-OX (PDB code: 1OEM) were used for the accessible surface area calculation. The accessible surface areas for the amino acids of PTP1B pTyr recognition loop are calculated using the program surface implemented in CCP4 suite[29].

**Reporting Summary.** Further information on research design is available in the Nature Research Reporting Summary linked to this article.

## Data availability

The structures of reduced PTP1B (PDB code: 2HNQ) and PTP1B-OX (PDB code: 1OEM) were used for the accessible surface area calculation. The MS data in Supplementary Tables 1 and 2 will be made available in the PRoteomics IDEntifications database.

## References

26. Zougman, A., Selby, P. J. & Banks, R. E. Suspension trapping (STrap) sample preparation method for bottom-up proteomics analysis. *Proteomics* **14**, 1006–11010 (2014).
27. Ross, P. L. et al. Multiplexed protein quantitation in Saccharomyces cerevisiae using amine-reactive isobaric tagging reagents. *Mol. Cell. Proteom.* **3**, 1154–1169 (2004).
28. Perkins, D. N., Pappin, D. J., Creasy, D. M. & Cottrell, J. S. Probability-based protein identification by searching sequence databases using mass spectrometry data. *Electrophoresis* **20**, 3551–3567 (1999).
29. Collaborative Computational Project, N. The CCP4 suite: programs for protein crystallography. *Acta Crystallogr. D* **50**, 760–763 (1994).

## Acknowledgements

We thank H. Fu for providing the 14-3-3ζ plasmid. This research was supported by the National Institutes of Health grant no. HL138605 and the American Heart Association grant no. 17GRNT33700265 to B.B. and National Institutes of Health grant no. GM55989 to N.K.T. B.B. is also grateful for support from the following foundations: the Heart and Stroke Foundation of Canada and SUNY Research Foundation. B.B. is an FRQS Research Scholar and A.B. was the recipient of a scholarship from the FRQS.

## Author contributions

A.D.L., A.B., S.M.C., A.K., G.C., S.H.M.R. and B.B. performed experiments and analyzed data. K.D.R. and D.J.P. acquired and analyzed MS data. S.J.K. performed structural analysis and modeling. F.Z. and R.J.L. acquired and analyzed SPR data. N.K.T. and B.B. wrote the manuscript.

## Competing interests

The authors declare no competing interests.

## Additional information

**Supplementary information** is available for this paper at https://doi.org/10.1038/s41589-019-0433-0.

**Correspondence and requests for materials** should be addressed to B.B.

**Reprints and permissions information** is available at www.nature.com/reprints.